JOURNAL OF GEOPHYSICAL RESEARCH, VOL. 86, NO. A7, PAGES 5519–5531, JULY 1, 1981

# Escaping Nonthermal Continuum Radiation

W. S. KURTH, D. A. GURNETT, AND R. R. ANDERSON

*Department of Physics and Astronomy, The University of Iowa, Iowa City, Iowa 52242*

New observations by the ISEE 1 plasma wave receiver reveal heretofore unreported details of the nonthermal continuum radiation from the earth. In particular, the higher frequency escaping component shows temporal and spectral features which are quite different from those of the lower frequency trapped emission. The higher frequency component is often clearly separated in frequency from the trapped component and high resolution spectrograms show that the escaping radiation consists of numerous narrowband emissions which drift slowly in frequency with time. The higher frequency component also exhibits greater temporal and spatial variability in both amplitude and frequency although the temporal variations are still quite smooth when compared to the more intense and higher frequency auroral kilometric radiation. Evidence is presented which clearly shows a direct connection between intense electrostatic emissions near the upper hybrid frequency and the escaping continuum radiation and strongly suggests the latter electromagnetic emission is generated through mode coupling with the upper hybrid waves. The new ISEE observations of the escaping continuum radiation from the earth strongly suggest a close correspondence with the newly reported narrowband kilometric radiation from Jupiter. Both emissions are relatively narrowband and show slow variations in amplitude with time. In both cases, the narrowband radiation lies above the trapped continuum radiation and below the intense extraordinary mode emissions (auroral kilometric radiation at the earth and decametric radiation at Jupiter). Evidence from both planets suggests the radiation is generated by intense electrostatic waves near the upper hybrid resonance frequency in the vicinity of the plasmapause at the earth and at the outer edge of the Io plasma torus at Jupiter.

## 1. INTRODUCTION

Terrestrial nonthermal continuum radiation was first detected in the frequency range of 30 to 110 kHz by *Brown* [1973] and in the range of 5 to 20 kHz by *Gurnett and Shaw* [1973]. Brown reported a power-law frequency dependence of the radiation, $f^{\gamma}$, with $\gamma \simeq -2.8$. The lower frequency cutoff near 30 kHz was apparently due to the propagation cutoff at the solar wind plasma frequency. Gurnett and Shaw detected a more intense component at lower frequencies with IMP 6 when the spacecraft was within the magnetospheric cavity. Since the local plasma frequency in the cavity is less than the solar wind plasma frequency the continuum radiation below 20–30 kHz is trapped within the cavity.

The terrestrial continuum radiation was characterized in detail by *Gurnett* [1975]. Gurnett provided details of the continuum radiation spectrum, separating the lower frequency trapped component from an escaping component at frequencies high enough to propagate freely out of the magnetosphere and into the solar wind. Using direction-finding techniques the escaping radiation was found to be generated just beyond the plasmapause from ~4 to ~14 hours local time. Further investigation into the source region via spatial intensity distributions indicated that while the intensity is remarkably constant throughout the magnetospheric cavity, a statistically significant maximum occurs in the local morning and afternoon between 5 and 8 earth radii ($R_E$). Estimates of the source size from direction-finding measurements of the escaping component indicated a relatively large source size (subtending a half angle of ~20° at $20 < R < 30\ R_E$). Gurnett also showed a close association between intense electrostatic bands near the electron plasma frequency (now identified as upper hybrid resonance emissions) and continuum radiation and argued that the electrostatic bands played an important role in the generation of continuum radiation.

*Frankel* [1973] proposed that the continuum radiation was generated by gyrosynchrotron radiation from energetic electrons in the outer radiation zone. The question of the continuum radiation generation mechanism was pursued by *Gurnett and Frank* [1976] in a paper which showed a correlated increase in 1 to 30 keV electrons and continuum radiation intensity. Gurnett and Frank argued that the injection of 1–30 keV electrons into the dawn outer radiation zone led to a coherent plasma instability (e.g., intense electrostatic waves near the upper hybrid resonance frequency, $f_{UHR}$) which, in turn, wave-wave coupled into the electromagnetic radiation. *Jones* [1976] suggested that the continuum radiation was generated by a linear conversion of *Z*-mode waves into *O*-mode electromagnetic radiation at the plasma frequency. *Christiansen et al.* [1979*a*, *b*] suggested a nonlinear interaction between the upper hybrid waves and ULF waves may produce the continuum radiation. *Melrose* [1981], in a critique of the available theories, suggested that the most likely mechanism for the generation of continuum radiation involved the coalescence of upper hybrid waves with low frequency ion-cyclotron waves.

Nonthermal continuum radiation has since been observed in the Jovian magnetosphere [*Scarf et al.*, 1979; *Gurnett et al.*, 1979*b*] and a similar emission has been detected at Saturn [*Gurnett et al.*, 1981*a*, *b*]. Hence, continuum radiation appears to be a common astrophysical phenomenon. With the added interest generated by its occurrence in other magnetospheres, it becomes increasingly important to understand as much as possible about the emission by studying the phenomenon in greater detail and with improved instrumentation at the earth. The primary motivation for the present work results from the new ISEE observations which show that the escaping continuum radiation differs from the trapped component in several temporal and spectral characteristics. We will argue, however, that even though the new observations reveal important differences, the two components of the continuum radiation spectrum are most likely generated by the same mechanism and the observed differences can be explained by considering the effect the cavity has on the trapped portion. Having dem-



Paper number 1A0545.
0148-0227/81/001A-0545$01.00

onstrated the two components are actually closely related through the source mechanism, it will become apparent that the escaping component will be particularly useful in the study of both the trapped and escaping components since the escaping radiation has not been modified by repeated reflections within the magnetospheric cavity.

A secondary objective of this study is to look for analogies with the radio spectra of other planetary magnetospheres, particularly Jupiter. The study of the radio spectra of two or more magnetospheres helps to break the study of the individual emissions into more well-defined classifications. The discovery of general features present in more than one planetary radio spectrum or lack thereof will eventually lead to a better understanding of not only the nonterrestrial radiation, but also the earth's own emissions as well.

The new continuum radiation observations were made by the ISEE 1 plasma wave experiment which is described in detail by *Gurnett et al.* [1978]. In addition to a high-time resolution 20-channel spectrum analyzer which covers the frequency range from 5.6 Hz to 311 kHz, the ISEE 1 plasma wave experiment contains a sweep-frequency-receiver and a wideband analog receiver which provided the data essential for these new observations. The sweep frequency receiver, which has good frequency and temporal resolution, covers the frequency range from 100 Hz to 400 kHz in 128 logarithmically spaced narrowband channels which are sequentially sampled. A complete spectral scan is obtained every 32 s. Each channel has a dynamic range of about 80 dB. The wideband analog receiver on ISEE 1 is an automatic-gain-control (AGC) receiver with selectable 10-kHz or 40-kHz bandwidths and 8 selectable baseline frequency ranges from nearly DC to 2 MHz. Particularly important in this study are bands beginning at 0, 31.25 and 62.5 kHz. The wideband analog receiver provides excellent temporal and spectral resolution.

The ISEE 1 orbit is highly eccentric with the initial apogee at 22.6 $R_E$ and perigee at 1.1 $R_E$ and an inclination of 30°. The spacecraft spin axis is nearly perpendicular to the ecliptic plane. The primary sensor utilized in this study is the long (215 m tip-to-tip) electric dipole antenna extended perpendicular to the spin axis.

## 2. Observations of Escaping Nonthermal Continuum Radiation

In this section we shall present observations of the amplitude, spectrum, temporal fluctuations, and source region of escaping nonthermal continuum radiation. Throughout, we shall compare these new observations with previously published findings in order to verify the identification of the radiation studied here and also to point out the significant new details present in these observations. It is hoped that the additional information gleaned from this study will lead to a much better understanding of the source of the radiation.

### *a. Spectral and Temporal Characteristics of Escaping Continuum Radiation*

This study will rely on the use of the sweep-frequency-receiver data to characterize the escaping continuum radiation, to contrast it with the trapped continuum radiation, and separate it from auroral kilometric radiation. Plates 1 and 2 provide representative examples of escaping nonthermal continuum radiation and a discussion of these examples will establish a solid foundation upon which more detailed analyses may be based. The plates are in the form of frequency-time spectrograms with the abscissa being time and the ordinate frequency. The electric field spectral density at each frequency-time point is represented by a color code. Dark blue in the plates represents the floor of the receiver dynamic range and red represents the upper limit of the dynamic range. The color bar provided at the right of each plate shows the relation between color and electric field spectral density in units of $V^2$ $m^{-2}$ $Hz^{-1}$.

Plate 1 is from an inbound pass on April 5, 1978, at ~1–2 hours magnetic local time. The escaping continuum radiation is evident in the frequency range ~40–100 kHz from ~0110 up to 1220 UT when the spacecraft encountered the plasmapause. The escaping continuum radiation is characterized by narrow bands lasting for hours which slowly drift up or down in frequency. A higher frequency emission near 200 kHz between 1000 and 1225 UT is also identified as escaping continuum radiation. The escaping radiation is accompanied at lower frequencies by trapped continuum radiation between ~7 and 25 kHz and at higher frequencies by auroral kilometric radiation between ~100 and 400 kHz.

One useful landmark usually apparent in the sweep-frequency-receiver displays is the band at the upper hybrid resonance frequency, $f_{UHR}$, which sweeps from about 20 kHz at 1100 UT to 400 kHz at 1245 UT in Plate 1. We usually associate the region where this band exhibits the greatest rate of change of frequency (1225 UT) with the plasmapause since this represents the largest density gradient along the spacecraft trajectory in the inner magnetosphere. It is apparent in Plate 1, then, that the escaping continuum radiation can be detected all along the spacecraft trajectory except inside the plasmasphere. The lower frequency cutoff of the trapped continuum radiation is approximately the local electron plasma frequency, $f_p^-$, and this cutoff provides another useful landmark which when coupled with the UHR band near the plasmapause provides a density profile of the magnetosphere along the spacecraft trajectory.

Plate 1 shows obvious differences between the appearance of the escaping continuum radiation and that of trapped continuum radiation and auroral kilometric radiation. The escaping component is relatively narrowbanded and drifts slowly up and down in frequency. The diagonal mottled appearance is due to the beat between the sample period and spin period and is indicative of a spin-modulated signal. There are fluctuations in intensity of the escaping radiation over time scales of about an hour.

The trapped continuum radiation is approximately the same intensity as the escaping component but appears to have less spectral structure than the escaping component. The trapped component exhibits a smooth variation in intensity versus frequency from the lower cutoff near $f_p^-$ to the apparent upper limit. *Gurnett* [1975] associated this upper limit with the plasma frequency in the solar wind. Hence, the explanation for the trapped continuum radiation is based on the fact that the radiation is reflected at the magnetopause if the wave frequency is less than $f_p^-$ in the solar wind.

The auroral kilometric radiation in Plate 1 is quite distinct from both components of the continuum radiation. The higher frequency emission is much more intense, at times, than the continuum radiation and also much more variable in intensity, sometimes increasing or decreasing by several orders of magnitude on time scales of ~1 min. Hence, the appearance of the kilometric radiation is dominated by 'vertical' structure in the sweep-frequency-receiver displays, i.e., domi-

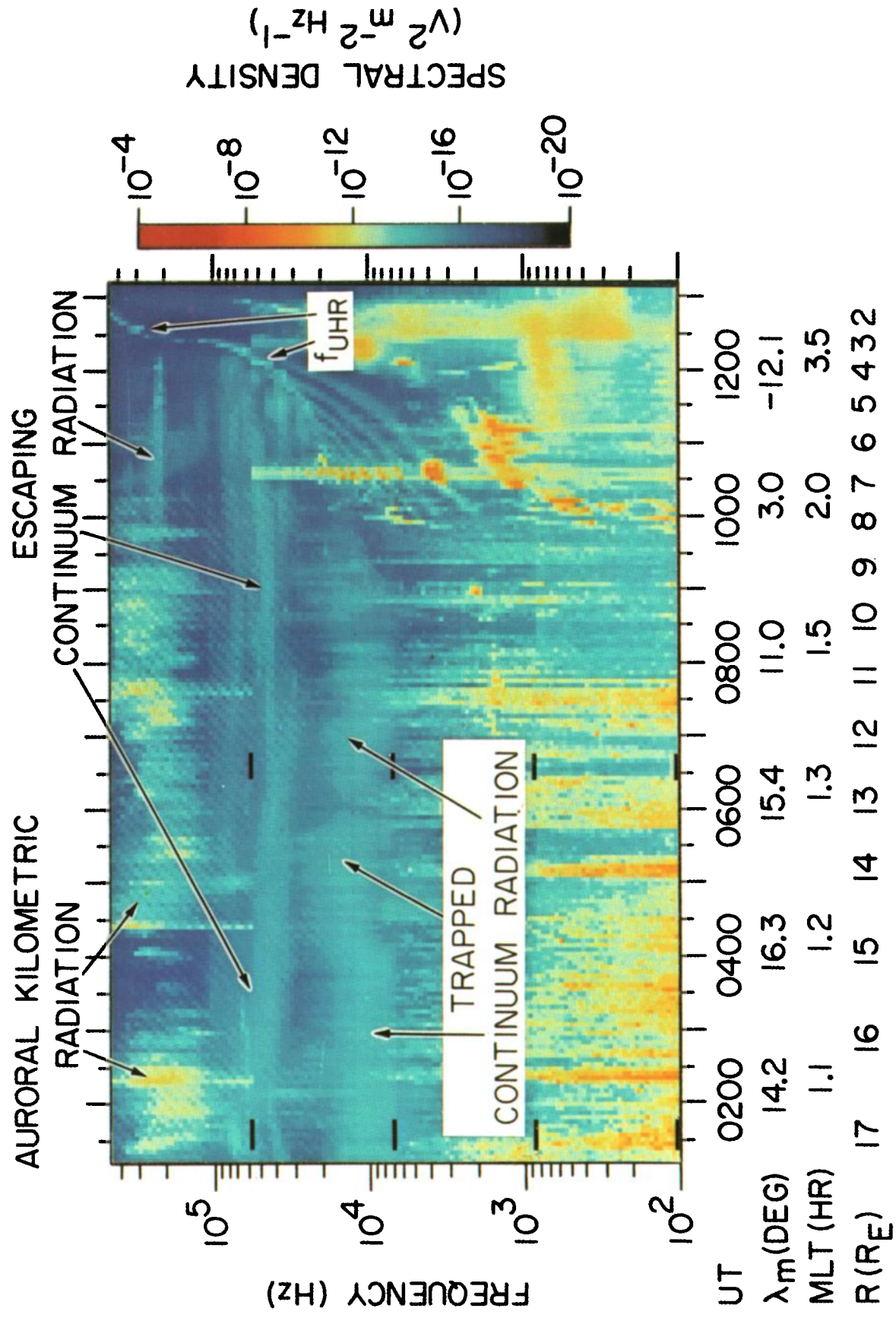


Plate 1. A frequency-time display of the ISEE 1 sweep-frequency-receiver data for the inbound pass on April 5, 1978. The color-coding scheme defined by the color bar at the right relates color to spectral densities such that blue represents weak wave intensities and red represents intense waves. This plate illustrates the relatively narrowband escaping continuum radiation which is well separated from both the trapped continuum radiation and intense auroral kilometric radiation.

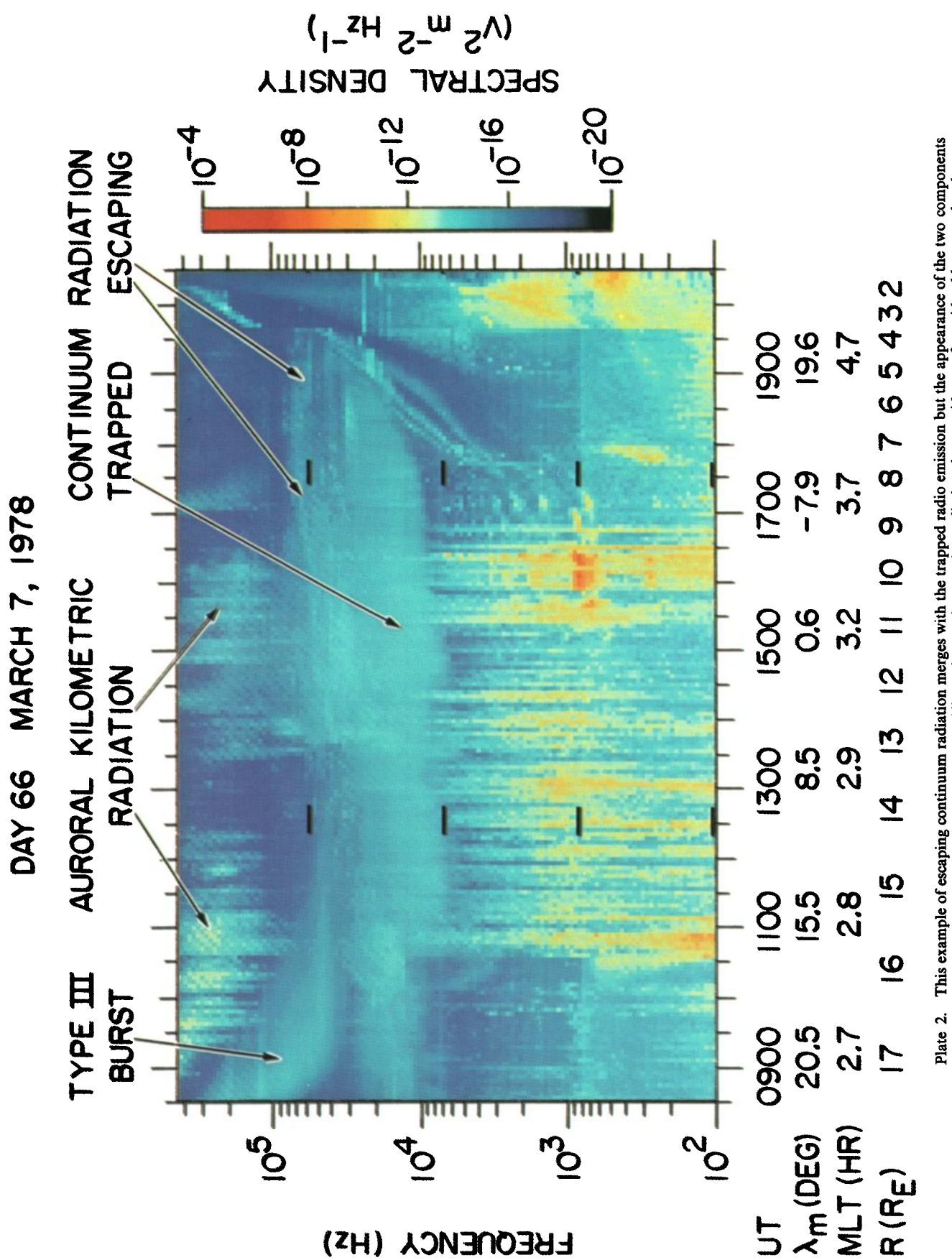


Plate 2. This example of escaping continuum radiation merges with the trapped radio emission but the appearance of the two components is strikingly dissimilar. The trapped emission is quite diffuse whereas the escaping radiation shows evidence of considerable narrowband spectral structure.

nated by temporal variations, whereas the escaping continuum radiation shows predominantly 'horizontal' structure, i.e., dominated by spectral variations.

Another example of escaping continuum radiation is shown in Plate 2. This case is interesting because the emission appears to merge with the trapped component when it is first observed near 1400 UT on March 7, 1978, but by 1700 UT there is an obvious gap between the diffuse trapped radiation and the banded escaping emission. Near the beginning of this pass a solar type III radio burst can be seen sweeping down from a few hundred kHz to ~50 kHz. Notice the very smooth and diffuse temporal and spectral character of the type III burst compared to the escaping continuum radiation. Hence, it is quite easy to distinguish the two phenomena. The detection of the type III burst demonstrates that waves at frequencies greater than ~50 kHz can escape from the magnetosphere.

The observations shown in Plates 1 and 2 provide considerable evidence that the waves studied here are, indeed, electromagnetic radiation and not the thermal electrostatic noise studied by *Hoang et al.* [1980]. The escaping continuum radiation consists of narrowband emissions which are often strongly spin modulated. The thermal electrostatic noise is a broadband emission and is not strongly spin modulated. The thermal noise is most intense just above the cutoff at the local plasma frequency [*Hoang et al.*, 1980]. The bands of escaping continuum radiation shown in Plates 1 and 2 are usually at frequencies much greater than $f_p^-$ (often near $10f_p^-$) and show little or no tendency to follow local variations in the plasma frequency in either the magnetosphere or solar wind. Observations shown below will reveal even more detailed frequency-time structure which should not be observed in association with thermal electrostatic noise. Further, the amplitudes of some of the emissions in Plates 1 and 2 exceed those expected for the Hoang effect by several orders of magnitude. It is virtually certain, therefore, that the radiation studied here is not the thermal electrostatic noise studied by *Hoang et al.* [1980].

Further details of the spectral character of the escaping continuum radiation can be found in the wideband analog receiver data. A particularly illustrative example is shown in Figure 1. The format of this figure is again that of a frequency-time diagram, but with a linear frequency scale and a white-to-black intensity scale. The receiver which provides these data has an automatic-gain-control circuit which adjusts the gain as the input signal intensity varies. Hence, the amplitudes are uncalibrated in an absolute sense. The dynamic range for any one spectral sweep shown is about 20 dB with black representing the most intense signals.

Figure 1 shows the nearly simultaneous occurrence of both trapped and escaping continuum radiation and auroral kilometric radiation. The escaping component observed between ~0525:30 and 0528 UT and between 20 and 30 kHz is characterized by numerous narrowband emissions which slowly drift in frequency. (The discontinuous change in the spectrum between ~0527:00 and 0527:36 is caused by another experiment's active control of the antenna and is not a natural phenomenon.) Trapped continuum radiation can be seen over most of the time period shown between 5 and 20 kHz. The trapped emission is very diffuse and structureless in frequency. The apparent abrupt changes in intensity, particularly after 0528:10 UT are artifacts caused by the AGC circuitry being affected by more intense signals below 5 kHz, probably broadband electrostatic noise. The lower frequency limit of the auroral kilometric radiation spectrum is evident between 0522:30 and 0525:30 UT at about ~27 kHz. The kilometric radiation is characterized by tones which rapidly rise or fall in frequency as reported by *Gurnett et al.* [1979*a*].

The higher resolution observations shown in Figure 1 confirm the results of the study of the sweep-frequency-receiver data and show that the escaping radiation is more highly structured in frequency than the trapped component. The intense, rapidly rising and falling tones of auroral kilometric radiation clearly separate it from the continuum spectrum and preserve the 'vertical' structure seen in the sweep-frequency-receiver displays.

It is useful to study further examples of the escaping continuum radiation in high resolution to search for clues to the source and origin of the emission. Figure 2 shows two widely differing examples of the emission. In the lower panel from December 29, 1977, the escaping radiation consists of pairs of extremely narrowband emissions separated by ~1.0–1.5 kHz. A banded structure in the trapped continuum radiation was reported by *Gurnett and Shaw* [1973] but the band spacing seldom, if ever, matched the local electron cyclotron frequency. The gyrofrequency at 0140 UT on December 29, 1977, is 715 Hz and clearly does not match the spacing of the bands in the lower panel of Figure 2. (The magnetic field data used to derive the local gyrofrequency are 1-min averages from the ISEE data pool tape. See *Russell* [1978] for a description of the magnetometer.) This result suggests two ideas concerning the source of the emission. First, the source is a remote one, probably located at a geocentric radial distance of ~8–9 $R_E$ where $f_g^-$ ~1 kHz, perhaps near the magnetopause. Second, in order to explain the extremely narrow bands, the source must be fairly compact so that characteristic frequencies in the source region, e.g., the gyrofrequency, do not vary by a large factor over the region of emission. There is evidence in the plasma wave data for this day that the solar wind density was elevated and upper hybrid bands at ~70 kHz near the magnetopause are possible and could provide the source of the radio emissions in this example.

A distinct character of escaping continuum radiation is evident in the upper panel of Figure 2 from December 28, 1977. This case shows numerous discrete tones lasting for only a few seconds each. These features also are undoubtably intimately involved in the source of the emission. *Gurnett and Shaw* [1973] also reported discrete structures in high resolution frequency-time displays of trapped continuum radiation observed by IMP 6. Figure 3 is an example from ISEE 1 showing both discrete tones (near 2200 and 2230 UT) and banded emissions in the spectrum of trapped continuum radiation. The observance of banded and discrete structures in both the escaping and trapped continuum radiation components provides highly suggestive evidence that the two components may have the same or at least similar sources.

It is interesting to compare spectra from the ISEE 1 sweep-frequency-receiver with those shown by *Gurnett* [1975]. The ISEE spectrum shown in the top panel of Figure 4 was selected from an event where the escaping radiation spectrum merged rather smoothly with the trapped continuum spectrum. This spectrum is qualitatively similar to those shown by Gurnett. The division indicated by shading in the spectrum between the two components comes from an analysis of the sweep-frequency-receiver frequency-time displays similar to Plates 1 and 2 which distinguishes between the diffuse appearance of the trapped emission and the structured appearance of

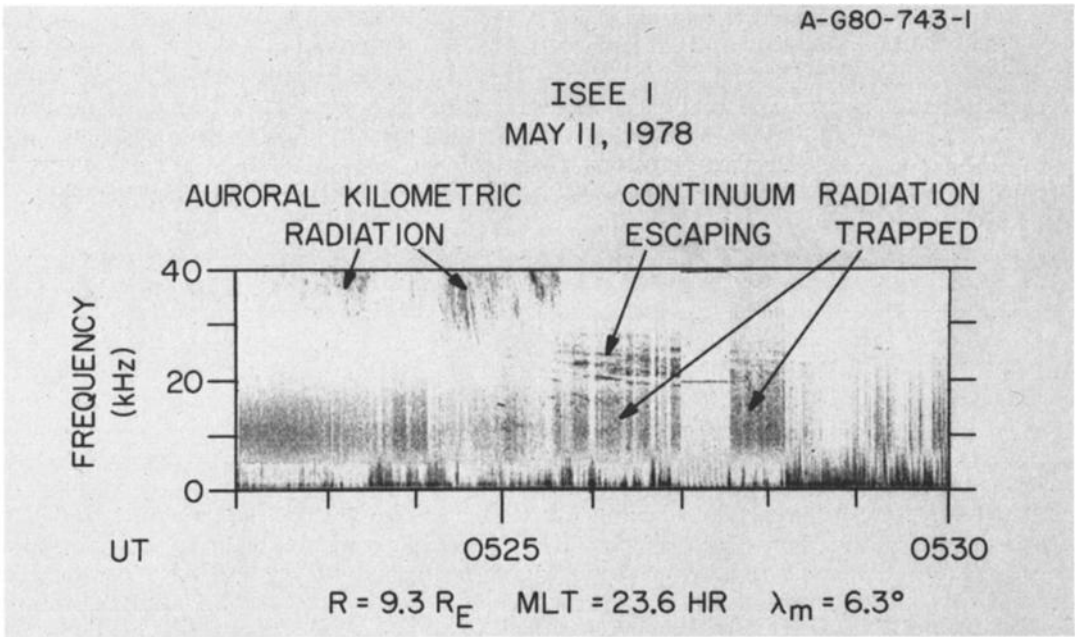


Fig. 1. A high resolution frequency-time spectrogram showing clear differences in the dynamic spectra of escaping and trapped continuum radiation and auroral kilometric radiation. Notice the narrowband features in the escaping continuum radiation which drift very slowly in time in contrast with the nearly structureless spectral character of the trapped emission.

the escaping radiation. The escaping continuum radiation spectra are generally more spiky and less continuous than those of the trapped emission.

To verify that our analysis of the qualitative character of the frequency-time spectrograms has provided a reasonable break-point between the trapped and escaping continuum components in Figure 4, we have obtained the solar wind density taken by IMP 7 simultaneously with the spectrum shown in the top panel of Figure 4. The electron number density in the solar wind was found to be 13 $cm^{-3}$ (A. J. Bame and J. T. Gosling, personal communication, 1981) corresponding to a solar wind plasma frequency $f_p$(SW) = 32.4 kHz. This fre-

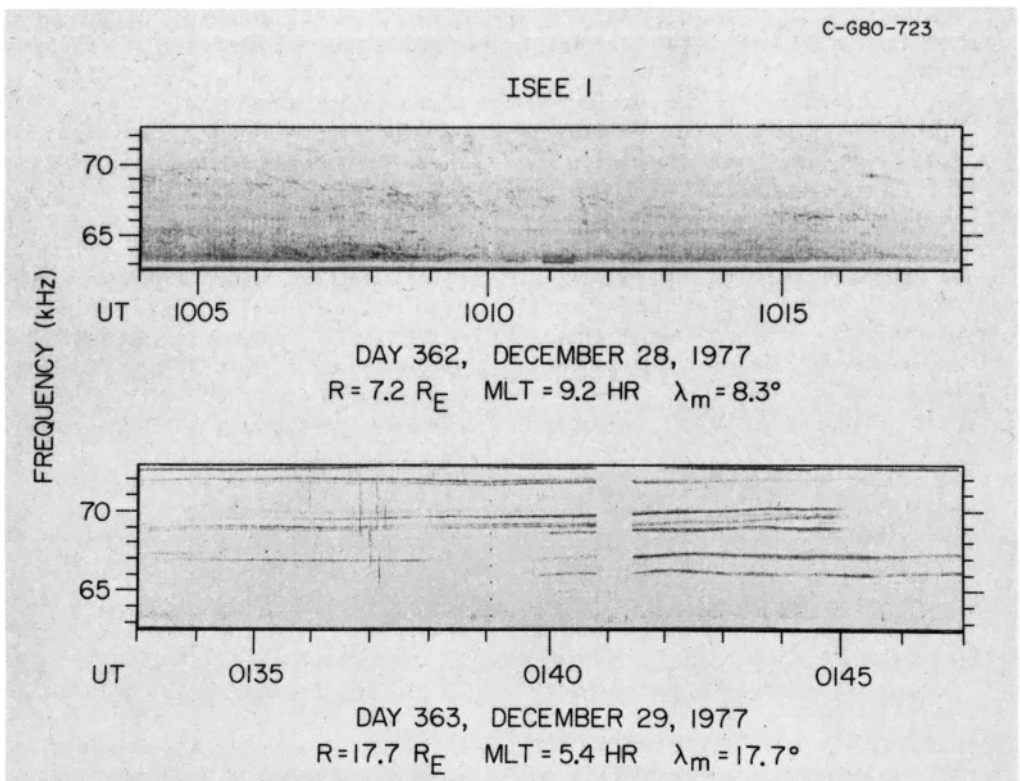


Fig. 2. Two examples of escaping continuum which show discrete and banded features, similar to structure seen within the trapped continuum radiation dynamic spectra observed with IMP 6.

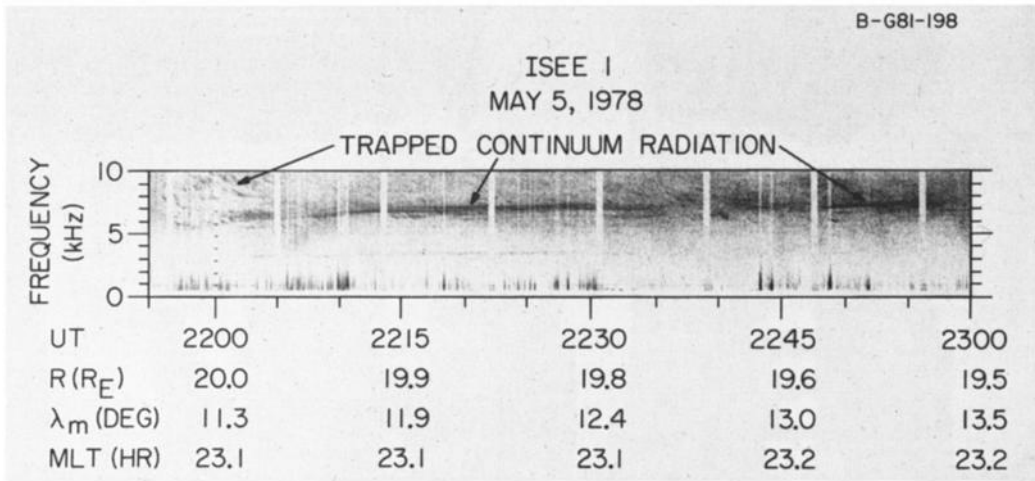


Fig. 3. An example of trapped continuum radiation which consists of both discrete and banded structures similar to those observed in the escaping component.

quency is labeled in the upper panel of Figure 4 and agrees almost exactly with the division between the trapped and escaping components shown on the basis of the plasma wave spectrum.

The spectrum in the upper panel of Figure 4 is qualitatively and quantitatively in agreement with those shown by *Gurnett* [1975]. A glance at Plate 1, however, would indicate that much different looking spectra also exist. The lower panel in Figure 4 shows an example of continuum radiation spectrum taken when the escaping component is well separated from the trapped emission and is quite intense. The example in the bottom panel of Figure 4 leads to the impression that the escaping continuum radiation might well be considered a separate and distinct feature in the earth's radio spectrum and not simply a portion of the continuum radiation spectrum. We have again shown the solar wind plasma frequency, $f_p$(SW) = 15.6 kHz, for the March 9, 1978, spectrum based on a solar wind electron density of 3 $cm^{-3}$ as measured by IMP 8 (A. J. Bame and J. T. Gosling, personal communication, 1981). Once more, there is a close correspondence between the solar wind plasma frequency and the frequency at which the spectrum shifts from the trapped to the escaping component.

We close this section by noting that in some cases the detailed frequency-time spectrograms suggest a common source for the trapped and escaping continuum radiation whereas in other cases the two components appear to be separate and distinct features of the terrestrial radio spectrum. We shall discuss this paradox and offer a solution in the Discussion section.

### b. *Source Region of Escaping Continuum Radiation*

*Gurnett* [1975] carried out direction-finding measurements on both the escaping and trapped continuum radiation and found a source at morning-to-afternoon local times between 3 and 8 $R_E$ for the escaping component. Since the trapped component undergoes repeated reflections at the magnetopause, direction-finding measurements of the trapped component could not provide a determination of the source region. *Christiansen et al.* [1979a] have also presented direction-finding measurements of the escaping continuum radiation which are consistent with a source location just beyond the plasmapause on the morning side. We have performed direction-finding measurements from ISEE 1 on escaping continuum radiation taking care to select examples which are clearly not contaminated either by auroral kilometric radiation or by trapped continuum radiation. Figure 5 is the result of a direction-finding survey similar to that done by *Gurnett* [1975]. The symbols mark the position of the spacecraft while the direction of arrival was being determined for frequencies ranging from 31.1 to 311 kHz. (See *Kurth et al.* [1975] and *Gurnett* [1975] for a summary of the direction-finding procedure.) Although there is a 180° ambiguity in the measurements, it was assumed the source was in the direction toward the earth. In cases where ambiguity was still possible, a line was extended in both directions from the symbol to represent the possible directions to the source. Superimposed on the figure is the source region from Figure 15 of *Gurnett* [1975] which indicated that the con-

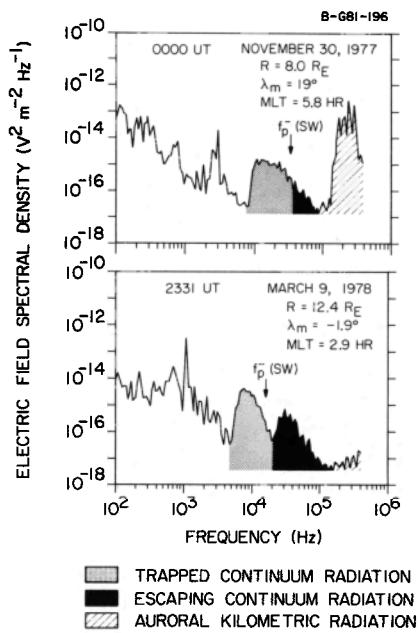


Fig. 4. Spectra obtained from ~3-min averages of the sweep-frequency-receiver output showing the relationship between the two continuum radiation components and auroral kilometric radiation. The top spectrum is similar to those shown by *Gurnett* [1975] and is not inconsistent with the concept of two similar components of the same radio emission feature. The bottom spectrum suggest two separate emission features comprise the continuum radiation spectrum.

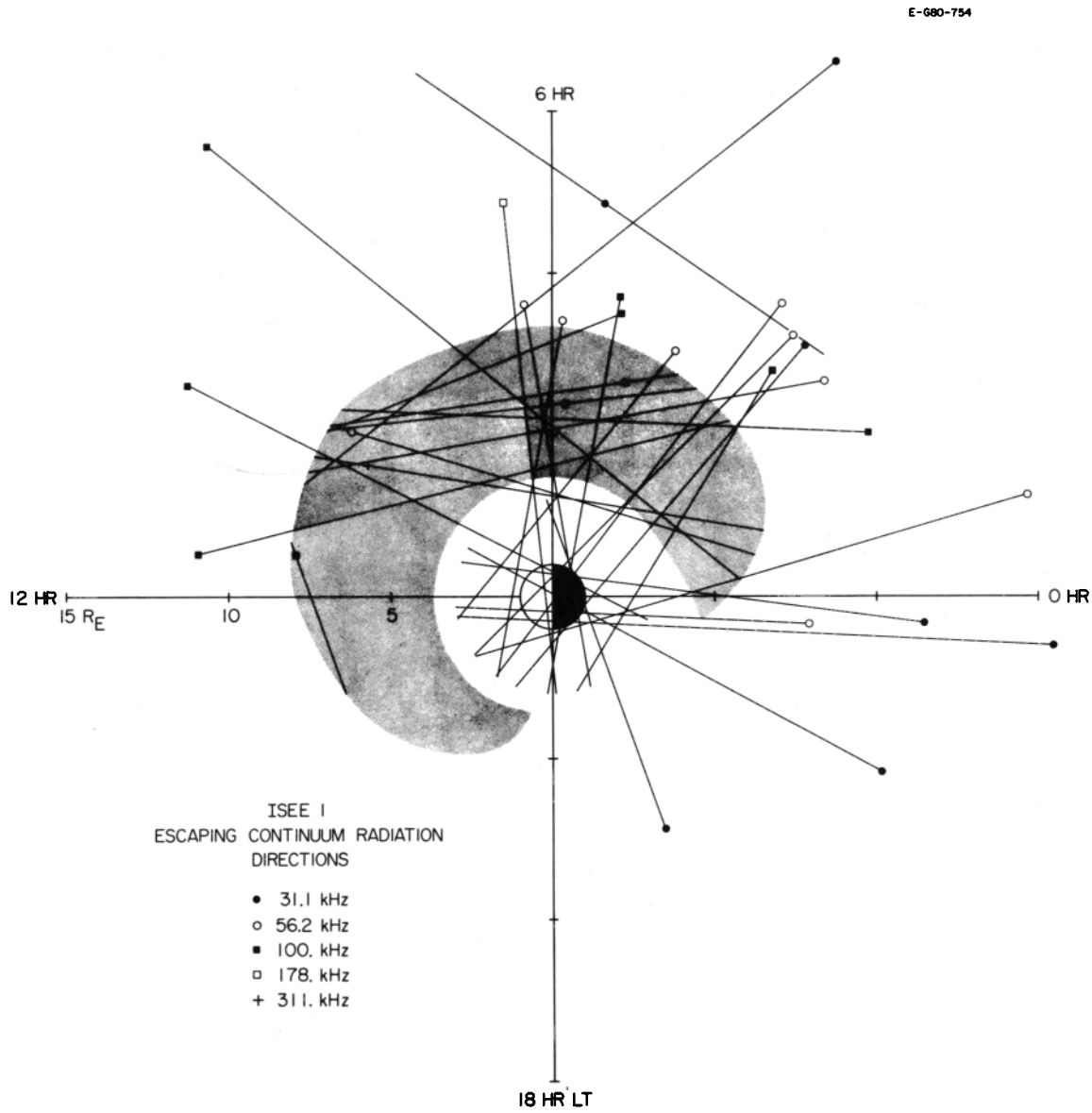


Fig. 5. Results of a direction-finding survey modeled after *Gurnett* [1975] which show general agreement with the source region found by *Gurnett* [1975] (shaded area). These results confirm the emissions studied by Gurnett and studied in this paper are the same phenomenon.

tinuum radiation source extended over a broad region beyond the plasmapause on the morning side of the earth. As can be seen in Figure 5, virtually all directions determined intersect the source region. Since we believe the emission studied here is the same as that studied by Gurnett it is not surprising that our results are consistent with the previous IMP 8 measurements. On the other hand, without the shaded region in Figure 5 to guide the eye, the results of the direction-finding survey are not very conclusive.

We supplement the direction-finding survey with a study of the occurrence of escaping continuum radiation as a function of spacecraft position in radial distance and local time. The portions of ISEE 1's trajectory which are plotted in Figure 6 represent times when a clear signature of the escaping continuum radiation is evident in the output of the sweep-frequency-receiver. This survey represents an entire year of observations; hence, a complete survey of local time is assured. The data set used was comprised of partial passes of the spacecraft from perigee to about 17 $R_E$; hence, the outer limit of observation is an artifact of the data set used, and not a radial distance limit of observation. Notice that escaping continuum radiation is most often observed during local morning, and particularly between about 0 and 7 hours local time. This result supports the conclusion that the source of continuum radiation is located primarily in the local morning beyond the plasmapause. The high density plasmasphere would block observations made by a near-equatorial spacecraft in the local afternoon and evening if the source were in the local morning. The region of ISEE 1 observations of escaping continuum radiation shown in Figure 6 clearly demonstrates the emission studied here is different from the $2f_p^-$ radiation from the bow shock mentioned by *Gurnett* [1975] and studied in detail by *Hoang et al.* [1981].

We conclude on the basis of the above remote sensing techniques and the more complete study of *Gurnett* [1975] that the primary source of the escaping nonthermal continuum is lo-

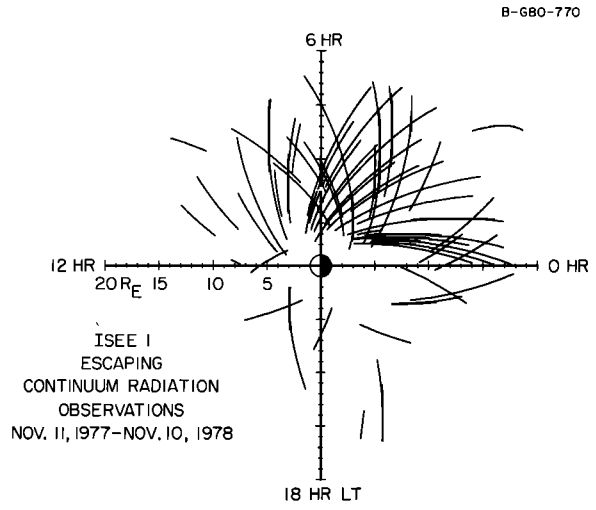


Fig. 6. A study of the region where escaping continuum radiation was observed by ISEE 1 over a one-year interval of time. Note that the outer limit of observation is not real but imposed by the data set used in the survey. The survey is consistent with a local morning source as determined by direction-finding measurements.

cated just beyond the plasmapause in the local morning region of the magnetosphere. There is more evidence supporting this particular source region, if one assumes, as suggested by *Gurnett* [1975], *Jones* [1976], *Christiansen et al.* [1979*a*, *b*], *Kurth et al.* [1979*b*], and *Melrose* [1981], that the continuum radiation is generated by some mechanism involving intense electrostatic waves near $f_{UHR}$. *Christiansen et al.* [1978], *Gough et al.* [1979], and *Kurth et al.* [1979*b*] showed electrostatic waves at intensities $\gtrsim 1$ mV m$^{-1}$ near $f_{UHR}$ are common features of the region just beyond the equatorial plasmapause ($3 \lesssim R \lesssim 7\ R_E$). No apparent local time asymmetry in the occurrence of the intense UHR bands favoring the local morning sector has been reported, however, this may be due to a lack of sufficient numbers of observations.

The magnetopause, however, should also be considered as a possible source of the continuum radiation. Analysis of the band spacing of the event shown in the bottom panel of Figure 2 led to the magnetopause as a likely source position for that particular event. Intense electrostatic waves near $f_{UHR}$ are relatively common in IMP 6 and ISEE plasma wave observations near the dayside magnetopause and these would be likely candidates for continuum radiation sources. (See the discussion of 'class 3' waves in *Hubbard et al.* [1979] and also *Curtis et al.* [1979].) Some of the direction-finding results shown herein are consistent with a mangetopause source, however, the occurrence study shown in Figure 6 suggests the morning plasmapause is the predominant source.

*Kurth et al.* [1979*b*] showed an example of intense upper hybrid waves near 4.3 $R_E$ at 5.6 hours local time which was apparently the source of nonthermal continuum radiation. Figure 16 of that paper showed that the intensity of the continuum radiation varied approximately at $(R - R')^{-2}$ where $(R - R')$ was the distance from the region of intense electrostatic waves and, thereby strongly suggested the electrostatic waves were participating in the generation of the continuum radiation.

Figure 7 is a similar but more revealing example relating the escaping continuum radiation to the electrostatic bands near $f_{UHR}$. In this frequency-time spectrogram the characteristic banded structure of continuum radiation is seen as ISEE 1 approaches the plasmapause. At about 6.4 $R_E$ near 1040:30 UT on December 28, 1977, the spacecraft encountered intense, narrowband electrostatic waves near $f_{UHR}$ similar to those studied by *Christiansen et al.* [1978], *Hubbard and Birmingham* [1978], and *Kurth et al.* [1979*b*]. In this region of space near the plasmapause the density gradient is relatively strong and the UHR bands occur when $f_{UHR} \simeq (n + 1/2)f_g^-$.

The most striking feature of the event in Figure 7 is the almost exact correspondence between the banded structure in the continuum radiation and the structure of the $(n + 1/2)f_g^-$ bands near $f_{UHR}$. The continuum radiation bands become stronger and more prominent as the spacecraft approaches the UHR bands and at ~1040:30 UT there is an abrupt transition from the continuum bands to the UHR bands. For this particular example, there is little doubt that the UHR bands are indeed the source of the escaping continuum radiation. It is obvious that the banded structure which has been shown to be characteristic of the escaping continuum radiation is directly related to the banded structure of the source electrostatic waves. The magnetic field strength from the ISEE data pool tape at 1040:30 UT is 146 nT giving an electron gyrofrequency of 4.1 kHz which is very close to the spacing of both the upper hybrid resonance bands and the continuum radiation bands. The close correspondence of the band spacing and the local magnetic field strength in this case is due to the fact that the spacecraft is in or very close to the source region. In the example shown in the bottom panel of Figure 2 where the band spacing is not the local gyrofrequency, the waves evidently propagate from a distant source.

More information about the source and source mechanism is apparent from Figure 7. The bandwidth of the continuum bands is typically ~2 kHz although each of the main emission bands are composed of numerous narrow bands with $\Delta f \sim 100$ Hz. This is suggestive of a lower frequency wave interacting nonlinearly with the upper hybrid waves to form the continuum radiation. Since the emission is not at $\sim 2f_{UHR}$ but centered almost exactly at $f_{UHR}$, the conservation laws indicate the third wave must be at a very low frequency, probably at $f \lesssim 100$ Hz. *Melrose* [1981] has suggested a generation mechanism which involves the coalescence of UHR bands with electrostatic ion cyclotron waves and *Christiansen et al.* [1978] have reported observations of intense waves in the ULF range during upper hybrid wave events, which could possibly correspond to the third wave in the nonlinear process. The observations would also be consistent with a linear conversion mechanism such as that of *Jones* [1976].

## 3. Discussion

The observations presented above serve to clarify our understanding of the character of the escaping continuum radiation but have led to a paradoxical situation concerning the relationship between the escaping continuum radiation and the trapped component. Hence, in the first portion of this section we will attempt to solve the problem of whether the two components are, indeed, related and, if so, how. In the second portion of this section we shall compare the new observations of the terrestrial escaping continuum radiation with observations of similar emissions from Jupiter.

### *a. Relationship Between Escaping and Trapped Continuum Radiation*

One of the new results of this paper is a more detailed description of escaping continuum radiation which in many

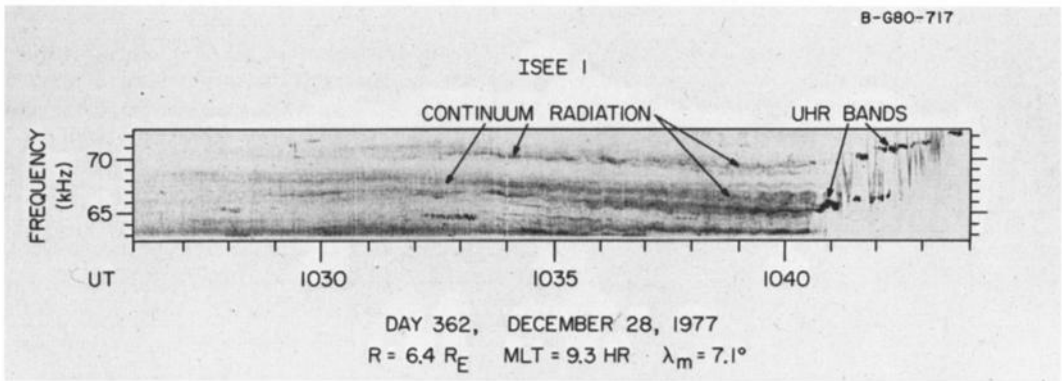


Fig. 7. A particularly revealing event which shows a direct connection between electrostatic UHR bands near the plasmapause and escaping continuum radiation with a rich banded spectrum. The bandwidth of the continuum radiation suggests a generation mechanism in which electromagnetic radiation is produced via a linear conversion process or by a nonlinear three-wave process.

ways separates it from the trapped radiation. Where earlier studies had suggested the higher frequency waves were different only in that they were not reflected at the magnetopause, this study shows a clear difference in the spectrum of the two components as shown in Plates 1 and 2 and also Figure 4. Clear distinctions between the two components can often be made with the aid of high resolution frequency-time spectrograms such as in Figure 1 which shows the complex spectral structure of the escaping continuum radiation in contrast with the diffuse nature of the trapped emission. Another difference between the two components is that the trapped continuum radiation fills the magnetospheric cavity almost uniformly while we have shown the preferential location for observing the escaping component to be in the local morning.

On the other hand, there are obvious similarities to the two components. The banded and discrete structures sometimes seen in trapped continuum radiation at the earth by *Gurnett and Shaw* [1973] and shown in Figure 3 are also seen in observations of the escaping radiation as shown in Figures 1 and 2. Similar banded structures are seen in the trapped continuum radiation at Jupiter [*Gurnett et al.*, 1979*b*]. Also, spectra such as those shown in the top panel of Figure 4 which suggest a more or less continuous transition from the trapped to the escaping portion of the spectrum indicate there is good reason to regard the two components as portions of a single radio emission.

We propose that even though new data presented in this paper suggests the escaping and trapped continuum radiation components are somewhat dissimilar in nature, they are generated via the same mechanism and all observed differences may be explained if one examines the effect of the reflections within the cavity on the trapped component. The presence of banded (and discrete) structures in both components is the key which leads to a common source mechanism. The discussion of Figure 7 could equally well apply to an example of trapped continuum radiation.

The differences in spectral character noted here can be largely explained by applying the work of *Barbosa* [1981] to terrestrial trapped continuum. Barbosa argued that movement of the cavity walls leads to a diffusion in frequency of continuum radiation trapped in the Jovian magnetosphere. Therefore, a monochromatic tone would be spread in frequency after a large number of reflections off the walls of the magnetospheric cavity. Hence, we may argue that the diffuse nature of the trapped continuum radiation is due to frequency diffusion as a result of multiple reflections off the magnetospheric walls. Also, since the UHR bands are observed to occur over a broad range of frequencies from as low as 10 kHz to at least 178 kHz, the superposition of waves impinging on the spacecraft from a large number of discrete sources within the magnetosphere via multiple reflections will result in a diffused spectrum. When banded structures are seen in the trapped spectrum we must assume the observing receiver is relatively close to the source or that the waves detected have experienced only a small number of reflections and, hence, have not diffused to a large extent.

The change in the character of the spectrum which occurs between the trapped and escaping components must be regarded as a transition from a regime in which the frequency diffusion discussed by *Barbosa* [1981] fills the band between the local plasma frequency and the solar wind plasma frequency with trapped radio waves to a regime where nearly monochromatic emissions escape from the magnetosphere without reflection. It is not clear that the emissions must occur over a continuous range of frequencies and, in fact, it is quite reasonable to expect local minima in the emission spectrum as in the bottom panel of Figure 4 because of the discrete character of the UHR source. There are also examples of the converse situation where escaping emission bands lie at a frequency such that the escaping and trapped spectra merge as is the case in Plate 2 and the top panel of Figure 4.

The observations of a uniformly filled cavity in the lower frequency range is a direct result of the confinement of the radio waves within the cavity. Even a source localized in the morning sector could illuminate the entire magnetospheric cavity via multiple reflections off the magnetopause. If the escaping component of the continuum radiation spectrum is due to discrete sources at frequencies above the solar wind plasma frequency, it may be necessary to re-evaluate the $Q$ factor of the magnetospheric cavity estimated by *Gurnett* [1975]. Gurnett assumed the entire continuum radiation spectrum was generated by a continuous source spectrum and used the ratio of the amplitudes of the trapped and escaping radiation to infer the $Q$ of the cavity. In view of the present situation with the escaping component generated by discrete, monochromatic sources with a complex frequency structure, it is more difficult to estimate the $Q$ of the cavity.

The observed differences in the trapped and escaping continuum radiation, then, may all be explained by considering the effect the cavity has on the trapped component but not on

the escaping component. The evidence suggesting a similar source mechanism is the basis for considering the two components parts of the same phenomenon. Hence, the escaping and trapped components are almost certainly intimately related.

The obvious advantage one may take of the situation is to generalize findings on the escaping component to the case of the whole continuum spectrum. That is, if we understand the generation mechanism of the escaping radiation, we may assume the trapped emission is generated in a similar manner. Since the cavity effects do not modify the escaping waves, studies of the higher frequency radiation are more direct and less confused by propagation effects than are measurements of the trapped radiation.

### b. *Relationship Between Terrestrial Escaping Continuum Radiation and Narrowband Jovian Kilometric Radiation*

It is useful to draw analogies between terrestrial phenomena and those from nonterrestrial magnetospheres in order to gain a broader insight into the phenomena in general and for the knowledge applicable to other astrophysical problems. *Kurth et al.* [1979*a*] described Jovian kilometric radiation as sometimes having the appearance of escaping continuum radiation from the earth and suggested that some of the lower frequency radiation from Jupiter was escaping continuum radiation generated within the Jovian magnetosphere. Largely on the basis of the latitudinal beaming effect reported for the Jovian kilometric radiation [*Gurnett et al.*, 1979*b*; *Warwick et al.*, 1979*b*; *Kurth et al.*, 1980*b*], *Jones* [1980] drew an analogy between terrestrial continuum radiation and Jovian kilometric radiation. We wish to pursue the analogy between continuum radiation at the earth and Jovian kilometric radiation but on a more restricted basis and for different reasons than utilized by Jones.

*Kaiser and Desch* [1980] have reported a separate component to the Jovian kilometric radiation spectrum which lies at generally lower frequencies than the broadband Jovian kilometric radiation [*Desch and Kaiser*, 1980] and has a narrow bandwidth ($\lesssim$40 kHz near 100 kHz). This narrowband Jovian kilometric radiation has many characteristics similar to those of the terrestrial escaping continuum radiation. The narrowband Jovian emission exhibits smooth and gradual variations in intensity as a function of time and frequency-time displays of the radiation [*Kaiser and Desch*, 1980] are very reminiscent of the banded structures seen in Plate 1.

The morphology of the Jovian and terrestrial radio spectra also show striking analogs if one interprets the narrowband kilometric radiation at Jupiter as escaping continuum radiation. At the earth, the frequency of the escaping radiation lies between the trapped continuum radiation and the more intense, highly variable auroral kilometric radiation. Similarly at Jupiter, the narrowband kilometric radiation lies above the trapped continuum radiation, and below the more intense and sporadic decametric radiation.

The analogy between Jovian narrowband kilometric radiation and terrestrial escaping continuum radiation extends to studies of the source region and generation mechanism of both emissions. Figure 8*a* summarizes the conclusions of this work and that of *Gurnett* [1975] that the terrestrial continuum radiation is generated beyond the dawn plasmapause particularly near the equator. The mechanism must directly involve the intense UHR bands found in this region of space and probably is similar to the mechanism of coalescence of the upper hybrid waves with lower frequency waves suggested by *Melrose* [1981].

Similarly, *Kaiser and Desch* [1980] have argued the source region for Jovian narrowband kilometric radiation must lie near the equator at the outer edge of the Io plasma torus near 8–9 $R_J$. *Kurth et al.* [1979*a*] suggested intense upper hybrid resonance waves observed in the plasma torus near the equator [*Scarf et al.*, 1979; *Warwick et al.*, 1979*a*; *Gurnett et al.*, 1979*b*; *Kurth et al.*, 1980*a*; *Birmingham et al.*, 1981] were a likely source for the Jovian kilometric radiation. Figure 8*b* shows those ideas on the source of Jovian narrowband kilometric radiation in schematic form.

The similarities in the morphology of Figures 8*a* and 8*b* are striking. The major difference is the substitution of the Io plasma torus at Jupiter in place of the plasmasphere at the earth. Another difference is that the Jovian emission is observed to come from different local times and in fact appears to emanate from a source which rotates around Jupiter at a rate ~3–5% less than that for rigid corotation [*Kurth et al.*, 1980*b*; *Kaiser and Desch*, 1980]. Since rotation is so much more important in the physics of the Jovian magnetosphere than at the earth, it is not surprising that corotation effects predominate over local time effects at Jupiter. The similarities in the source regions at the earth and Jupiter also extend to the magnetopause. *Gurnett et al.* [1979*b*] showed examples of continuum radiation in the Jovian magnetosphere with a distinct banded structure not far from intense electrostatic bands near $f_{UHR}$ at the magnetopause which are very reminiscent of possible sources near the terrestrial magnetopause.

We stress the importance of limiting the analogy between terrestrial escaping continuum radiation and Jovian kilometric radiation to the narrowband Jovian emission and not the broadband emission. The spectral and temporal behavior of broadband Jovian kilometric radiation [*Desch and Kaiser*, 1980; *Kurth et al.*, 1980*b*] are quite dissimilar to the character of the terrestrial continuum radiation. Further, ray tracing and polarization arguments place the source for the broadband Jovian kilometric radiation in the low altitude auroral regions [*Green and Gurnett*, 1980; *Desch and Kaiser*, 1980] in contrast to the equatorial position inferred by *Kaiser and Desch* [1980] for the narrowband source. The analogy made by *Jones* [1980] rested heavily on the latitudinal beaming effect (or equatorial shadow zone) reported for the Jovian emission. This effect holds only for the broadband Jovian kilometric radiation and not the narrowband radiation as can be seen clearly in Figure 2 of *Warwick et al.* [1979*b*]. Contrary to the report by *Jones* [1980] of a latitudinal effect seen in the terrestrial continuum radiation, preliminary analysis of ISEE observations show no consistent dimunition of continuum radiation intensity near the magnetic equator and little or no evidence of beaming of the continuum radiation away from the magnetic equator as predicted by Jones.

## 4. CONCLUSIONS

This paper has added a body of detailed information to the information which was already available on the earth's continuum radiation and the escaping component in particular. These observations have shown that there are substantial qualitative differences in the spectrum and appearance of the two components, but that most of these differences may be explained by considering the effect of the cavity on the trapped radiation. Most importantly, the source mechanism for both

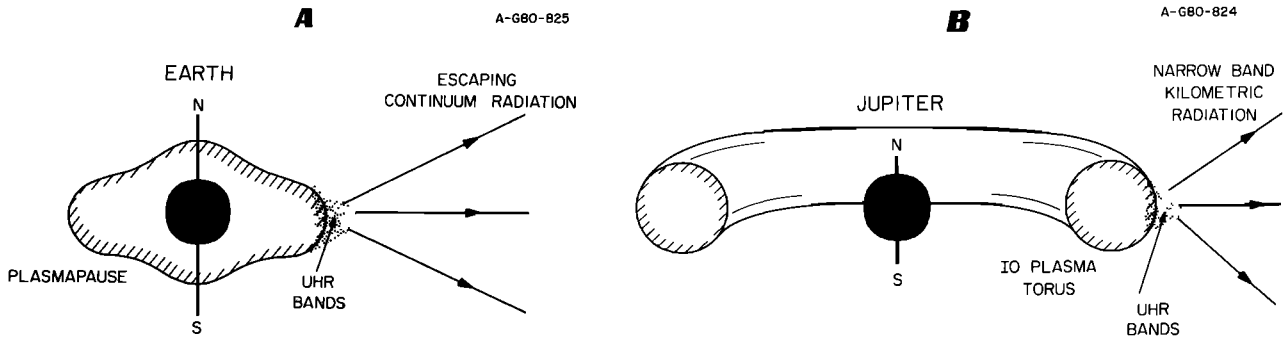


Fig. 8. (*a*) A schematic representation showing the escaping continuum radiation generation region just outside the plasmapause on the dawn side. The source region is the location of intense UHR bands which are fundamental to the generation mechanism. (*b*) An analogous view of the generation scheme of narrowband kilometric radiation at Jupiter. The primary difference is that the plasmasphere at the earth is replaced by the Io plasma torus at Jupiter in this model.

components is apparently the same and observations shown herein have demonstrated an almost unmistakable connection between electrostatic waves near $f_{UHR}$ just outside the plasmapause (and probably near the magnetopause) and the escaping continuum radiation. These observations support the suggestion by *Gurnett* [1975], *Jones* [1976], *Christiansen et al.* [1979*a*], and *Kurth et al.* [1979*b*] that UHR bands may be important in the generation of the trapped continuum radiation. Further, the structure in the continuum radiation very close to the source shown in Figure 7 implies that a mode coupling mechanism is most probable, and that the gyrosynchrotron mechanism proposed by *Frankel* [1973] probably is not of primary importance.

Arguments are also given above which suggest the Jovian narrowband kilometric radiation is very similar to the earth's escaping continuum radiation and may indeed be the same phenomena. The analogy extends to similarities in the source region and even the speculated emission mechanism in that the Jovian emission has been associated with UHR bands in or near the Io plasma torus. It is important to our understanding of both the terrestrial emission and the Jovian emission to see the similarities involved in a phenomenon associated with these two diverse magnetospheres. The similarity most likely lies in the microphysics of the upper hybrid resonance–$(n + 1/2)f_g^-$ instability and not so much in the gross morphology of the magnetospheres. It is quite likely that the banded electromagnetic radiation detected at Saturn [*Gurnett et al.*, 1981*a*, *b*] is similar in nature to the Jovian and terrestrial continuum radiation. If so, the implication is that continuum radiation is a fairly common astrophysical phenomenon and it is important to understand the generation mechanism as a fundamental process.

*Acknowledgments.* The authors would like to express their gratitude to M. Ashour-Abdalla for her interest in this research and her many useful comments and suggestions. We are also grateful to C. T. Russell for supplying magnetic field intensities used to calculate gyrofrequencies for some of the events studied and to the Los Alamos space plasma experiment team for providing solar wind electron densities from IMP 7 and 8 used in Figure 4. This research was supported by the National Aeronautics and Space Administration under contract NAS5-20093 with Goddard Space Flight Center, grants NGL-16-001-002 and NGL-16-001-043 from NASA Headquarters, and by the Office of Naval Research.

The Editor thanks M. P. Gough for his assistance in evaluating this paper.

## REFERENCES

Barbosa, D. D., Fermi-compton scattering due to magnetopause surface fluctuations in Jupiter's magnetospheric cavity, *Astrophys. J., 243,* 1076, 1981.

Birmingham, T. J., J. K. Alexander, M. D. Desch, R. F. Hubbard, and B. M. Pedersen, Observations of electron gyroharmonic waves and the structure of the Io torus, *J. Geophys. Res.*, in press, 1981.

Brown, L. W., The galactic radio spectrum between 130 kHz and 2600 kHz, *Astrophys. J., 180,* 359, 1973.

Christiansen, P. J., M. P. Gough, G. Martelli, J. J. Bloch, N. Cornilleau, J. Etcheto, R. Gendrin, C. Beghin, P. Decreau, and D. Jones, GEOS-1 observations of electrostatic waves, and their relationship with plasma parameters, *Space Sci. Rev., 22,* 383, 1978.

Christiansen, P. J., M. P. Gough, J. Etcheto, J. G. Trotignon, D. Jones, G. Belmont, and A. Roux, Observations of continuum radiation in the earth's magnetosphere, paper presented at the XVII IUGG/IAGA General Assembly, Int. Union of Geod. and Geophys./Int. Assoc. of Geomagn. and Aeron., Canberra, Australia, Dec. 3–14, 1979*a*.

Christiansen, P. J., M. P. Gough, G. Martelli, G. L. Wrenn, J. F. E. Johnson, and K. Rönnmark, Quasi-linear and nonlinear phenomena associated with strong electrostatic waves in the magnetosphere, paper presented at the XVII IUGG/IAGA General Assembly, Int. Union of Geod. and Geophys./Int. Assoc. of Geomagn. and Aeron., Canberra, Australia, Dec. 3–14, 1979*b*.

Curtis, S. A., C. S. Wu, and D. H. Fairfield, Electromagnetic and electrostatic emissions at the cusp-magnetosphere interface during substorms, *J. Geophys. Res., 84,* 898, 1979.

Desch, M. D., and M. L. Kaiser, The occurrence rate, polarization character, and intensity of broadband Jovian kilometric radiation, *J. Geophys. Res., 85,* 4248, 1980.

Frankel, M. S., LF radio noise from the earth's magnetosphere, *Radio Sci., 8,* 991, 1973.

Gough, M. P., P. J. Christiansen, G. Martelli, and E. J. Gershuny, Interaction of electrostatic waves with warm electrons at the geomagnetic equator, *Nature, 279,* 515, 1979.

Green, J. L., and D. A. Gurnett, Ray tracing of Jovian kilometric radiation, *Geophys. Res. Lett., 7,* 65, 1980.

Gurnett, D. A., The earth as a radio source: The nonthermal continuum, *J. Geophys. Res., 80,* 2751, 1975.

Gurnett, D. A., and L. A. Frank, Continuum radiation associated with low-energy electrons in the outer radiation zone, *J. Geophys. Res., 81,* 3875, 1976.

Gurnett, D. A., and R. R. Shaw, Electromagnetic radiation trapped in the magnetosphere above the plasma frequency, *J. Geophys. Res., 78,* 8136, 1973.

Gurnett, D. A., F. L. Scarf, R. W. Fredricks, and E. J. Smith, The ISEE-1 and ISEE-2 plasma wave investigation, *IEEE Trans. Geosci. Electron., GE-16,* 225, 1978.

Gurnett, D. A., R. R. Anderson, F. L. Scarf, R. W. Fredricks, and E. J. Smith, Initial results from the ISEE-1 and -2 plasma wave investigation, *Space Sci. Rev., 23,* 103, 1979*a*.

Gurnett, D. A., W. S. Kurth, and F. L. Scarf, Plasma wave observa-

tions near Jupiter: Initial results from Voyager 2, *Science, 206,* 987, 1979*b*.

Gurnett, D. A., W. S. Kurth, and F. L. Scarf, Plasma waves near Saturn: Initial results from Voyager 1, *Science, 212,* 235, 1981*a*.

Gurnett, D. A., W. S. Kurth, and F. L. Scarf, Narrowband electromagnetic emissions from Saturn's magnetosphere, submitted to *Nature,* 1981*b*.

Hoang, S., J.-L. Steinberg, G. Epstein, P. Tilloles, J. Fainberg, and R. G. Stone, The low-frequency continuum as observed in the solar wind from ISEE 3: Thermal electrostatic noise, *J. Geophys. Res., 85,* 3419, 1980.

Hoang, S., J. Fainberg, J.-L. Steinberg, and R. G. Stone, The $2f_p$ circumterrestrial radio radiation as seen from ISEE 3, *J. Geophys. Res.*, in press, 1981.

Hubbard, R. F., and T. J. Birmingham, Electrostatic emissions between electron gyroharmonics in the outer magnetosphere, *J. Geophys. Res., 83,* 4837, 1978.

Hubbard, R. F., T. J. Birmingham, and E. W. Hones, Jr., Magnetospheric electrostatic emissions and cold plasma densities, *J. Geophys. Res., 84,* 5828, 1979.

Jones, D., Mode coupling of Cerenkov radiation as a source of noise above the plasma frequency, in *The Scientific Satellite Programme During the International Magnetospheric Study,* edited by K. Knott and B. Battrick, p. 281, D. Reidel, Hingham, Mass., 1976.

Jones, D., Latitudinal beaming of planetary radio emissions, *Nature, 288,* 225, 1980.

Kaiser, M. L., and M. D. Desch, Narrow-band Jovian kilometric radiation: A new radio component, *Geophys. Res. Lett., 7,* 389, 1980.

Kurth, W. S., M. M. Baumback, and D. A. Gurnett, Direction-finding measurements of auroral kilometric radiation, *J. Geophys. Res., 80,* 2764, 1975.

Kurth, W. S., D. D. Barbosa, F. L. Scarf, D. A. Gurnett, and R. L. Poynter, Low frequency radio emissions from Jupiter: Jovian kilometric radiation, *Geophys. Res. Lett., 6,* 747, 1979*a*.

Kurth, W. S., J. D. Craven, L. A. Frank, and D. A. Gurnett, Intense electrostatic waves near the upper hybrid resonance frequency, *J. Geophys. Res., 84,* 4145, 1979*b*.

Kurth, W. S., D. D. Barbosa, D. A. Gurnett, and F. L. Scarf, Electrostatic waves in the Jovian magnetosphere, *Geophys. Res. Lett., 7,* 57, 1980*a*.

Kurth, W. S., D. A. Gurnett, and F. L. Scarf, Spatial and temporal studies of Jovian kilometric radiation, *Geophys. Res. Lett., 7,* 61, 1980*b*.

Melrose, D. B., A theory for the nonthermal radio continua in the terrestrial and Jovian magnetospheres, *J. Geophys. Res., 86,* 30, 1981.

Russell, C. T., The ISEE 1 and 2 fluxgate magnetometers, *IEEE Trans. Geosci. Electron., GE-16,* 239, 1978.

Scarf, F. L., D. A. Gurnett, and W. S. Kurth, Jupiter plasma wave observations: An initial Voyager 1 overview, *Science, 204,* 991, 1979.

Warwick, J. W., J. B. Pearce, A. C. Riddle, J. K. Alexander, M. D. Desch, M. L. Kaiser, J. R. Thieman, T. D. Carr, S. Gulkis, A. Boischot, C. Harvey, and B. M. Pedersen, Voyager 1 planetary radio astronomy observations near Jupiter, *Science, 204,* 995, 1979*a*.

Warwick, J. W., J. B. Pearce, A. C. Riddle, J. K. Alexander, M. D. Desch, M. L. Kaiser, J. R. Thieman, T. D. Carr, S. Gulkis, A. Boischot, Y. Leblanc, B. M. Pedersen, and D. H. Staelin, Planetary radio astronomy observations from Voyager 2 near Jupiter, *Science, 206,* 991, 1979*b*.

(Received January 22, 1981;
revised March 16, 1981;
accepted March 31, 1981.)